An Investigation to Document Morrow Reservoirs That Can Be Better Detected with Seismic Shear (S) Waves Than With Compressional (P) Waves

Final Report prepared for U.S. Department of Energy under
DOE Program Solicitation DE-PS26-99BC15146 entitled,
Technology Development with Independents

Visos Energy Corporation
Austin, Texas

Table of Contents

List of Figures

Introduction

Pennsylvanian-age Morrow reservoirs are a key component of a large fluvial-deltaic system that extends across portions of Colorado, Kansas, Oklahoma, and Texas. A problem that operators have to solve in some Morrow plays in this multi-state area is that many of the fluvial channels within the Morrow interval are invisible to seismic compressional (P) waves. This P-wave imaging problem forces operators in such situations to site infill, field-extension, and exploration wells without the aid of 3-D seismic technology.

The objective of this project was to develop and demonstrate seismic technology that can improve drilling success in Morrow plays. Current P-wave technology commonly results in 80-percent of Morrow exploration wells not penetrating economic reservoir facies. Studies at Colorado School of Mines have shown that some of the Morrow channels that are elusive as P-wave targets create robust shear (S) wave reflections (Rampton, 1995). These findings caused Visos Energy to conclude that exploration and field development of Morrow prospects should be done by a combination of P-wave and S-wave seismic imaging.

To obtain expanded information about the P and S reflectivity of Morrow facies, 9-component vertical seismic profile (9-C VSP) data were recorded at three locations along the Morrow trend. These data were processed to create P and S images of Morrow stratigraphy. These images were then analyzed to determine if S waves offer an alternative to P waves, or perhaps even an advantage over P waves, in imaging Morrow reservoir targets. The study areas where these field demonstrations were done are defined in Figure 1. Well A was in Sherman County, Texas; well B in Clark County, Kansas; and well C in Cheyenne County, Colorado.

Technology demonstrated at these sites can be applied over a wide geographical area and influence operators across the multi-state region spanned by Morrow channel plays. The scope of the investigation described here is significant on the basis of the geographical extent of Morrow

1

reservoirs, the number of operators that can be affected, and the importance of Morrow hydrocarbon reserves to the nation's economy.

Morrow Stratigraphy and Depositional Environment

The Morrow Formation is an asymmetrical wedge of Pennsylvanian-age sediments, generally less than 700 ft thick, that extends northwest-southeast from the Denver Basin in east-central Colorado into the Anadarko Basin of western Oklahoma. The sediments onlap pre-Pennsylvanian sediments along the ancient Amarillo-Wichita Mountains to form the southern boundary of Morrow deposition and wedge out onto the central Kansas Uplift to form their northern limit (fig. 1). To the northwest, the Morrow crosses the Las Animas Arch and extends into the Denver Basin. To the southeast, the Morrow thickens to as much as 3,000 ft or more in the Anadarko Basin.

The lower Morrow fills erosional lows in underlying pre-Pennsylvanian units, causing its thickness to vary over short distances. The dominant lithofacies are shallow marine sandstones, claystones, and limestones (fig. 2). The top of the lower Morrow is often marked by a sandy, skeletal limestone that can be as much as 200 feet thick (Swanson, 1979). The upper Morrow consists of claystone, sandstone, and discontinuous coarse conglomerates, with minor amounts of coal and thin limestone dispersed through the section.

The upper Morrow is bounded by the Atokan-age Thirteen Finger Limestone/Dolomite (fig.2). In some areas, this upper contact is an angular unconformity. A paleogeographic reconstruction of upper Morrow depositional environments is shown in Figure 1. Morrow deposition occurred in a low-accommodation basin, with the elevation of most of the middle to lower deltaic plain being only 50 to 60 feet above sea level (Swanson, 1979).

Known meander-belt areas are shown in Figure 1. Additional hypothetical channel systems are added to the figure to indicate the general depositional environment. Sediments were reworked
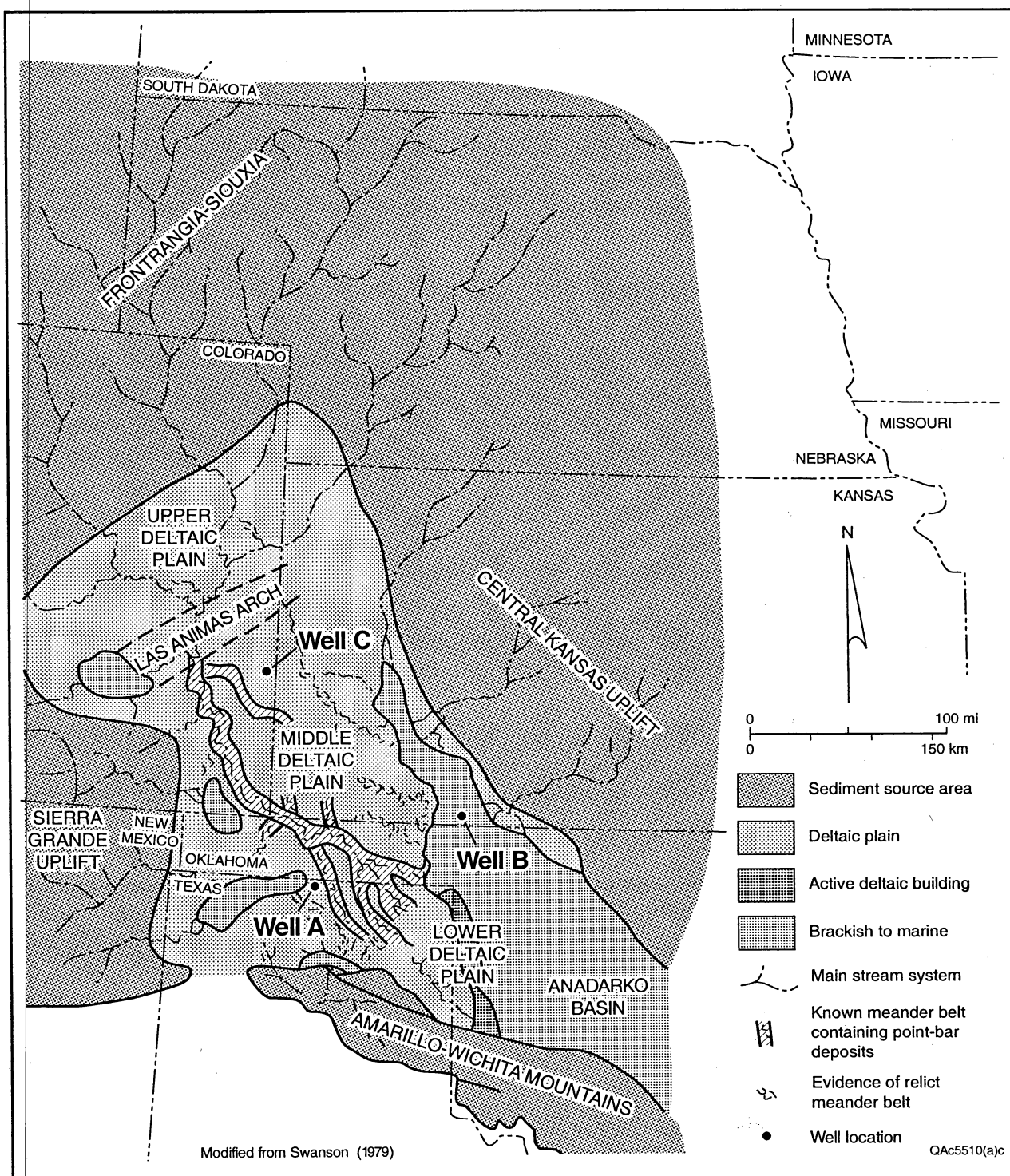
Figure 1. Location of demonstration wells A, B, and C. The background map shows key physiographic elements and depositional environments that existed when Morrow sediments were deposited (Modified from Swanson, 1979).

SP   Resistivity

Atokan	Thirteen Finger clayey limestones and dolomites	

Top of Morrow

Morrowan — Upper: Claystones, sandstones, conglomerates, coals, and thin limestones

Section exhibits variable fluvial-deltaic environments

Base of upper Morrow

Top of lower Morrow

Morrowan — Lower: Shallow marine sandstones, claystones, limestones, and sandy limestones

Base of Morrow

Mississippian: Chester limestones and shales

Misissippian or pre-Mississippian deposits
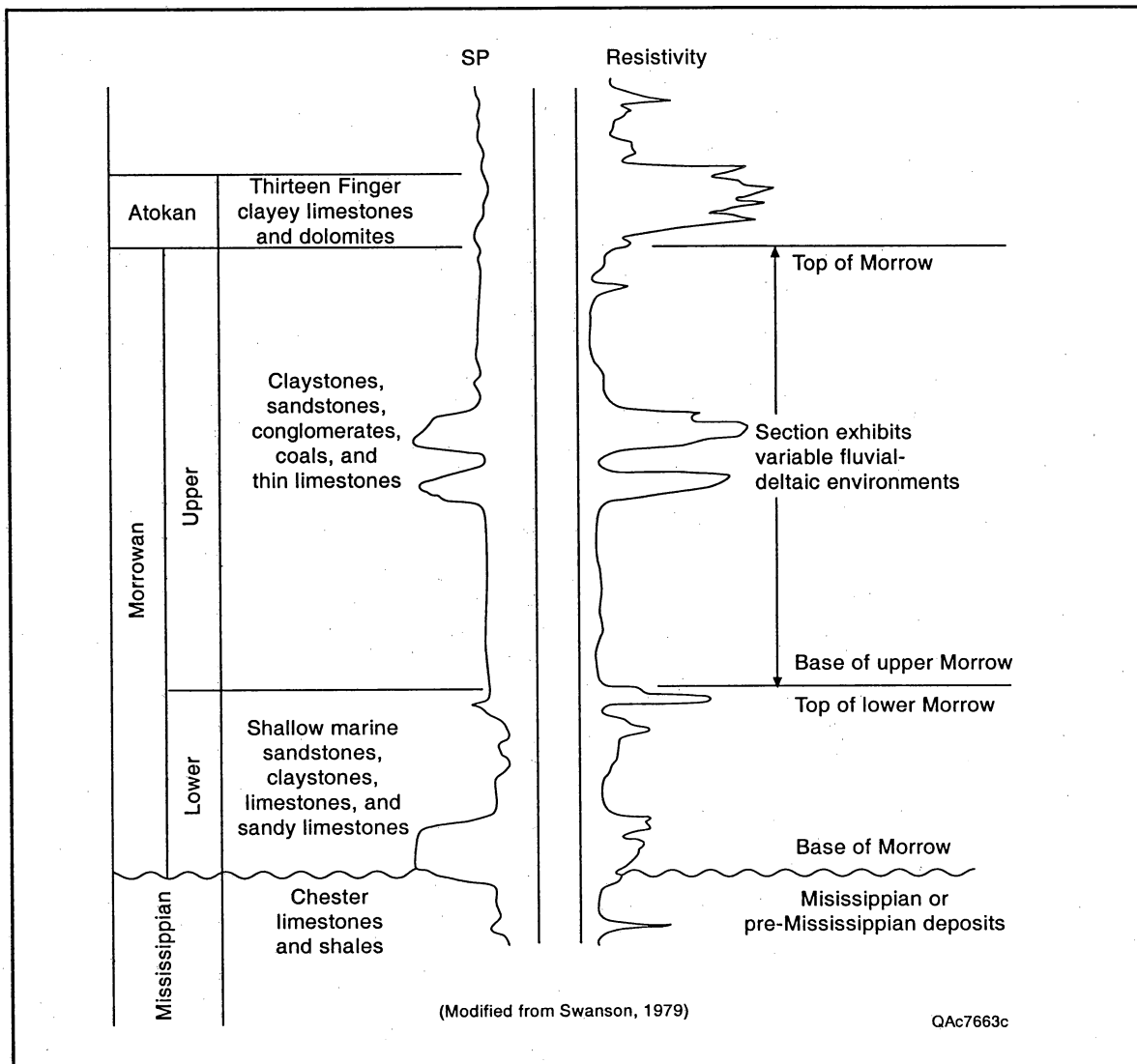
(Modified from Swanson, 1979)

QAc7663c

Figure 2. Type logs through Morrow stratigraphy (Taken from Swanson, 1979).

as these streams meandered back and forth across the upper delta plain. The depth of the Morrowan sea was not great, particularly in late Morrow time (Swanson, 1979). As a result, marine processes that contributed to sediment reworking and deposition appear to be small magnitude.
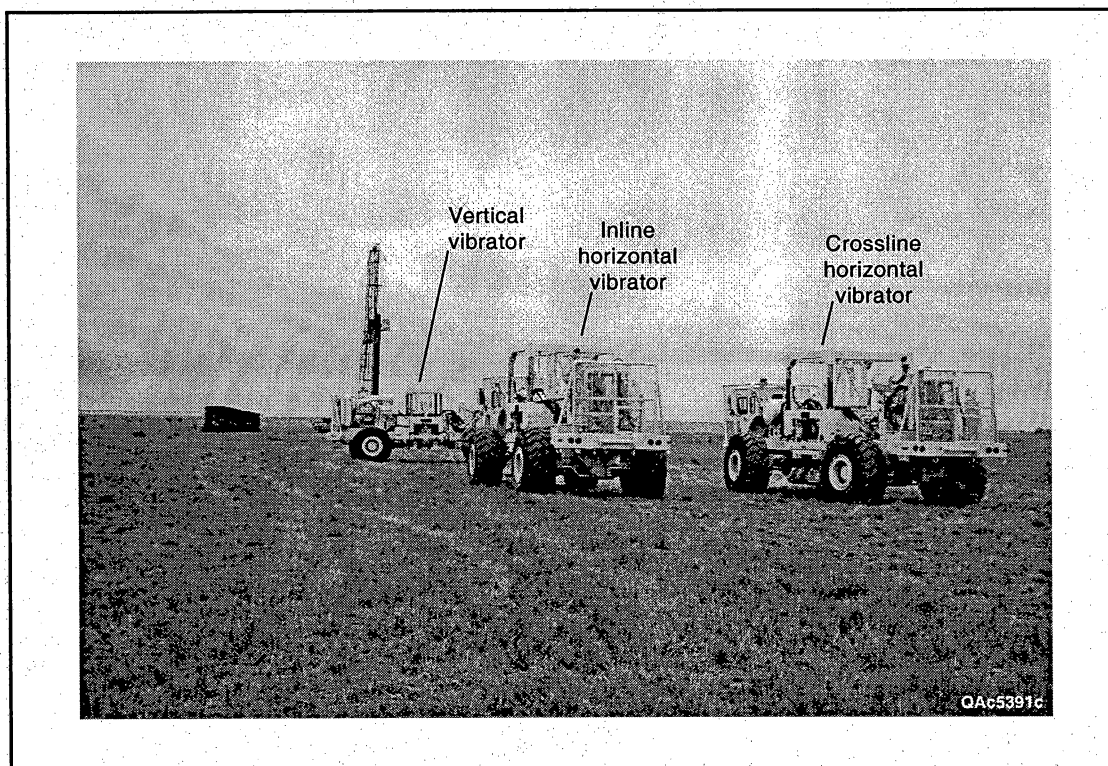
Figure 3. Orthogonal vector-wavefield sources used to generate 9C VSP

VSP Data Acquisition

Nine-component VSP (9-C VSP) data were acquired at three Morrow test well locations (fig. 1) using vertical arrays of 3-component (3-C) geophones and three distinct vector seismic sources: a vertical vibrator, an inline horizontal vibrator, and a crossline horizontal vibrator. These three vibrators were positioned a small offset distance from each vertical well to create a zero-offset recording geometry (fig. 3). The wavefield generated by each vibrator was recorded as a separate field record by the 3-C VSP geophones to create 9-C VSP data. At zero offset, a vertical vibrator creates a downgoing illumination wavefield with a strong P-wave component, and a horizontal vibrator creates a wavefield that has a strong, polarized S-wave component. These essential requirements for acquiring 9-C VSP data (3-C geophones and 3 orthogonal sources) are illustrated in Figure 4.
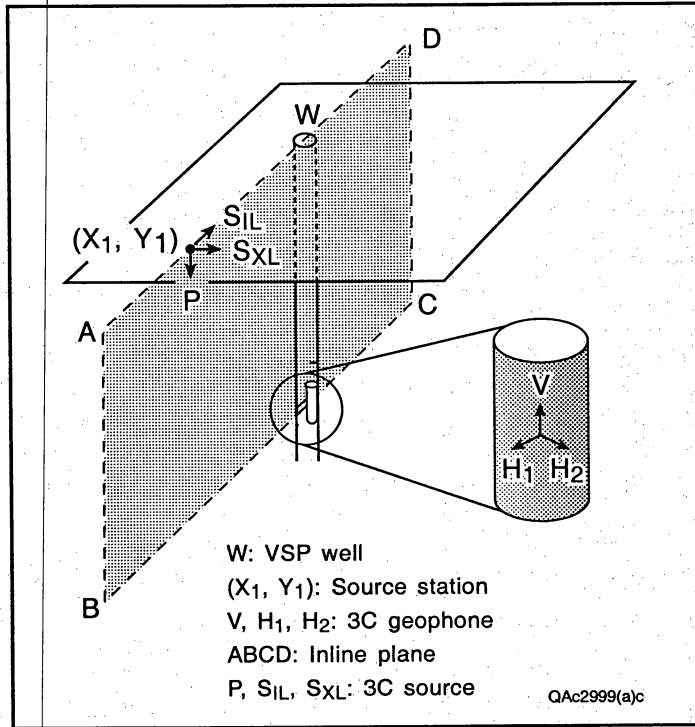
5

Figure 4. Basic geometry and key elements needed for 9C VSP data acquisition

W: VSP well
(X_1, Y_1): Source station
V, H_1, H_2: 3C geophone
ABCD: Inline plane
P, S_{IL}, S_{XL}: 3C source

QAc2999(a)c

In this figure, source vector P indicates the force vector applied by the vertical vibrator shown in Figure 3; S_{IL} is the force vector applied by the inline horizontal vibrator; and S_{XL} is the force vector produced by the crossline horizontal vibrator. In this VSP data-acquisition program, *inline* is defined as the direction from the source station to the vertical receiver station, which is the orientation direction of vertical plane ABCD in Figure 4. *Crossline* is defined as the direction perpendicular to inline, which would be the direction normal to plane ABCD.

Each downhole receiver station was occupied by a 3-C geophone comprised of a vertical sensor V and two orthogonal horizontal sensors H_1 and H_2 (fig. 4). For the vertical wells utilized in this study, vertical geophone V was always aligned in plane ABCD. H_1 and H_2 were oriented in different azimuth directions relative to plane ABCD at each downhole receiver station because of the tool spin that results when a downhole device such as a VSP sonde is suspended and operated by wireline.

6

Receiver Orientation

Downhole wireline-deployed tools spin as they are raised uphole because they are suspended on a twisted-wire cable that rotates about its longitudinal axis as the wireline is wound onto the cable spool. Because of this tool rotation, the azimuth orientation of horizontal geophones H_1 and H_2 (fig. 4) changes between adjacent depth stations as VSP data are recorded. No gyro tool was attached to the downhole receiver package used in this VSP data acquisition program, thus the orientations of the H_1 and H_2 sensors had to be determined from the seismic data that were recorded. We used the common industry procedure of recording P-wave first arrivals from a far-offset vertical vibrator to orient the horizontal elements of the 3-C VSP receiver at each depth station. This geophone orientation technique assumes that the P-wave first arrival from a far-offset source travels in the vertical plane that passes through the downhole geophone and surface source coordinates, which would be a plane similar to plane ABCD in Figure 4.

A two-step data coordinate transformation is required for proper receiver orientation, as illustrated in Figure 5. Panel 5a shows the orientation of the downhole geophone at the time when the VSP data were recorded, with X, Y, and Z being the orientation of the H_1, H_2, and V geophones, respectively. Horizontal geophone H_1 (x axis) is oriented at angle θ relative to the vertical plane that passes through the source and receiver coordinates.

The first coordinate transformation step is a right-handed rotation θ about the Z axis as shown in panel 5b. Angle θ is defined by mathematically rotating the H_1 and H_2 data in small angular increments (say 5 degrees) and determining which rotation angle maximizes the P-wave first arrival response on H_1 and minimizes the P-wave first arrival on H_2. After rotation, the new coordinates for receivers H_1, H_2, and V are X', Y', and Z', respectively (panel 5b).

The second step is a right-handed rotation $\emptyset$ of the V data and the new H_1' data about the new Y' axis (panel 5c). Angle $\emptyset$ is defined by mathematically rotating the V and H_1' data by small
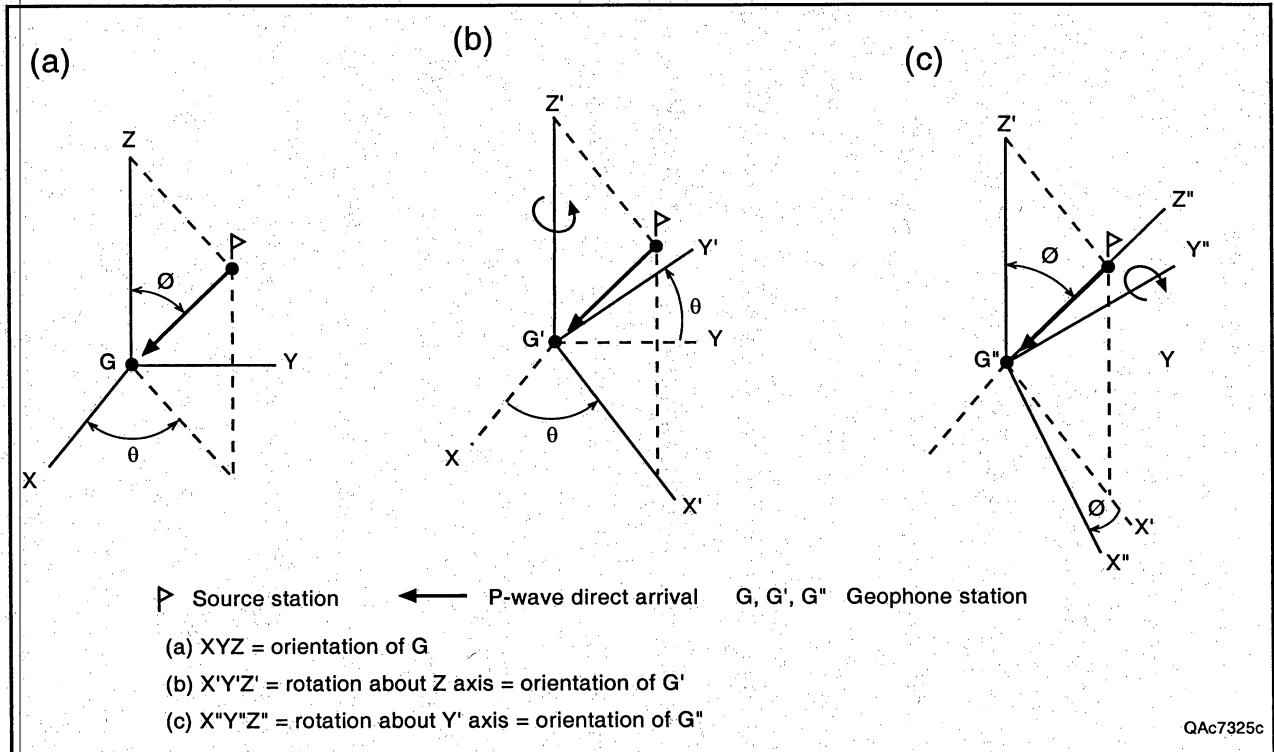
Figure 5. Rotation of 3-C VSP geophone to separate P, SV and SH wave modes

angle increments of 5 degrees or so until the P-wave first arrival is a maximum on V and a minimum on H_1'. The final orientation of receivers H_1, H_2, and V are now labeled X", Y", and Z", respectively (panel 5c).

This coordinate rotation technique points (mathematically) every V receiver directly at the far-offset source, positions every H_1 geophone in the vertical plane passing through the far-offset source and downhole receiver coordinates (which is plane X"Z" in panel 5c), and orients every H_2 geophone perpendicular to plane X"Z". The result is that all horizontal receivers throughout the vertical array are oriented in the same azimuth direction. Industry experience has shown that for VSP data acquisition in a simple horizontal-layer Earth, this geophone orientation technique of using P-wave first arrivals from a far-offset source is as reliable a method for orienting downhole geophones as is the directional information provided by a downhole gyro tool.
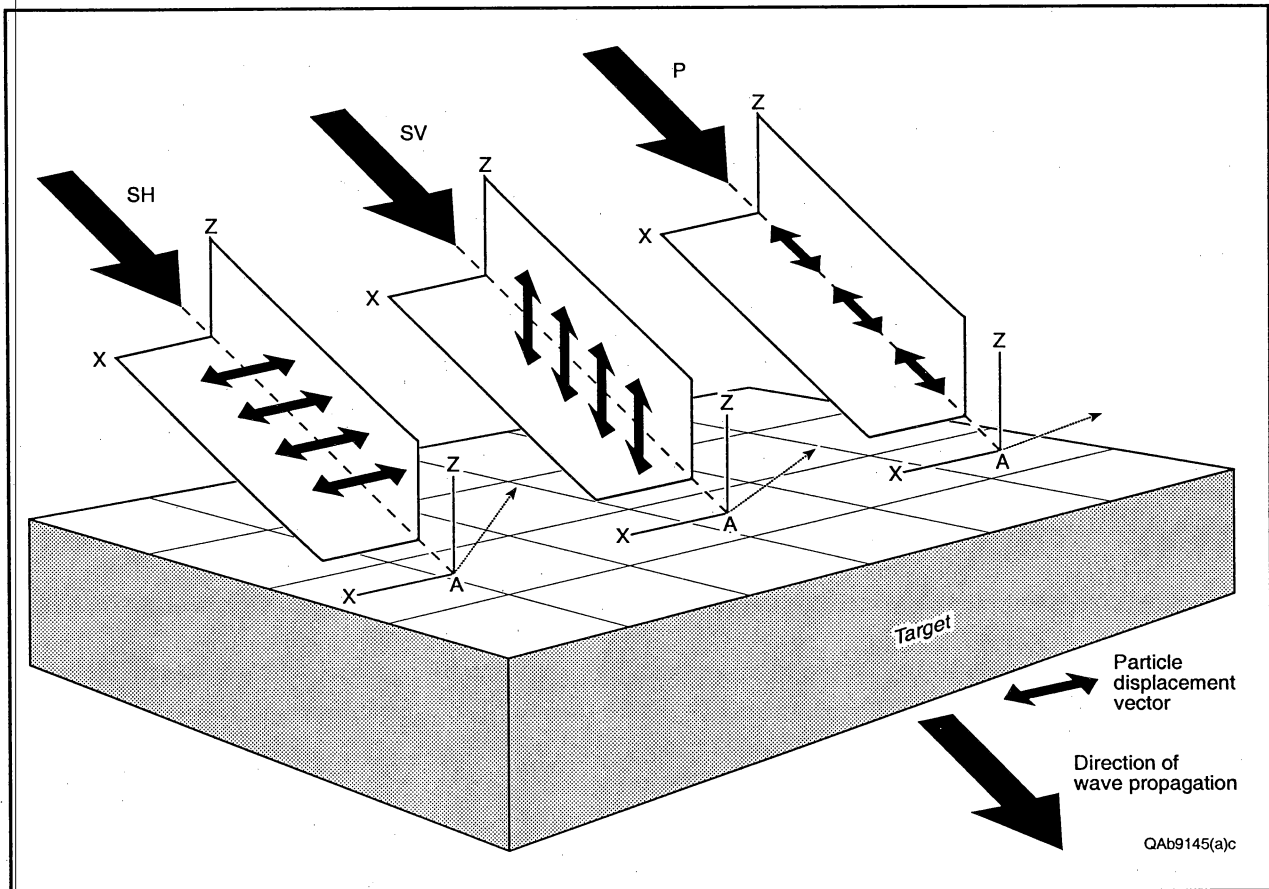
Figure 6. Distinctions among the particle-displacement vectors associated with the three fundamental modes, P, SH, and SV, that comprise vector-wavefield seismic data.

Wave Mode Separation

Three fundamental wave modes are required to define the full vector properties of a seismic wavefield, these being the compressional (P) mode, the horizontal shear (SH) mode, and the vertical shear (SV) mode. Key distinctions among these wave modes are the differences in the particle-displacement vector motions that they induce into the rock systems in which they propagate. The differing orientations of these particle displacement vectors with respect to the direction of wavefield propagation are illustrated in Figure 6.

9

The reason for recording 9-C VSP data (P-source, SH-source, and SV-source data) rather than 3-C VSP data (P-source data only) in this project is that 9-C VSP data allow all three fundamental wave modes (P, SH, SV) to be extracted and used for imaging. In contrast, 3-C VSP data do not contain SH modes, and SV images must be made from secondary SV data that are produced by P-to-SV mode conversions.

After the receiver rotation described in the preceding section is applied to 9-C VSP data, receiver V is oriented along the Z" axis of Figure 5c and captures the P-wave mode produced by the vertical vibrator in Figure 3. The rotation process orients receiver H_1 along the X" axis of Figure 5c and causes that receiver to record almost pure SV data generated by the inline vibrator shown in Figure 3. Receiver H_2 is oriented along the Y" axis (fig. 5c) and records almost pure SH data generated by the crossline vibrator shown in Figure 3.

VSP Recording Geometries

Map views of VSP source station positions used at demonstration wells A, B, and C are provided as Figures 7, 8, and 9, respectively. All receiver wells were vertical, thus receiver stations are stacked vertically beneath the well symbol shown on each map. At each study well, the three orthogonal sources shown in Figure 3 were stationed at the coordinates labeled *near offset*. The photograph in Figure 3 was taken as 9-C VSP data were being recorded in well A. Figure 9 shows the vibrator deployment used at demonstration well C. At each study well, one or two vertical vibrators were stationed at the coordinates labeled *far offset*. These far-offset sources created the critical P-wave first arrivals that were needed to rotate the downhole 3-C geophones to the same orientations at all receiver stations.
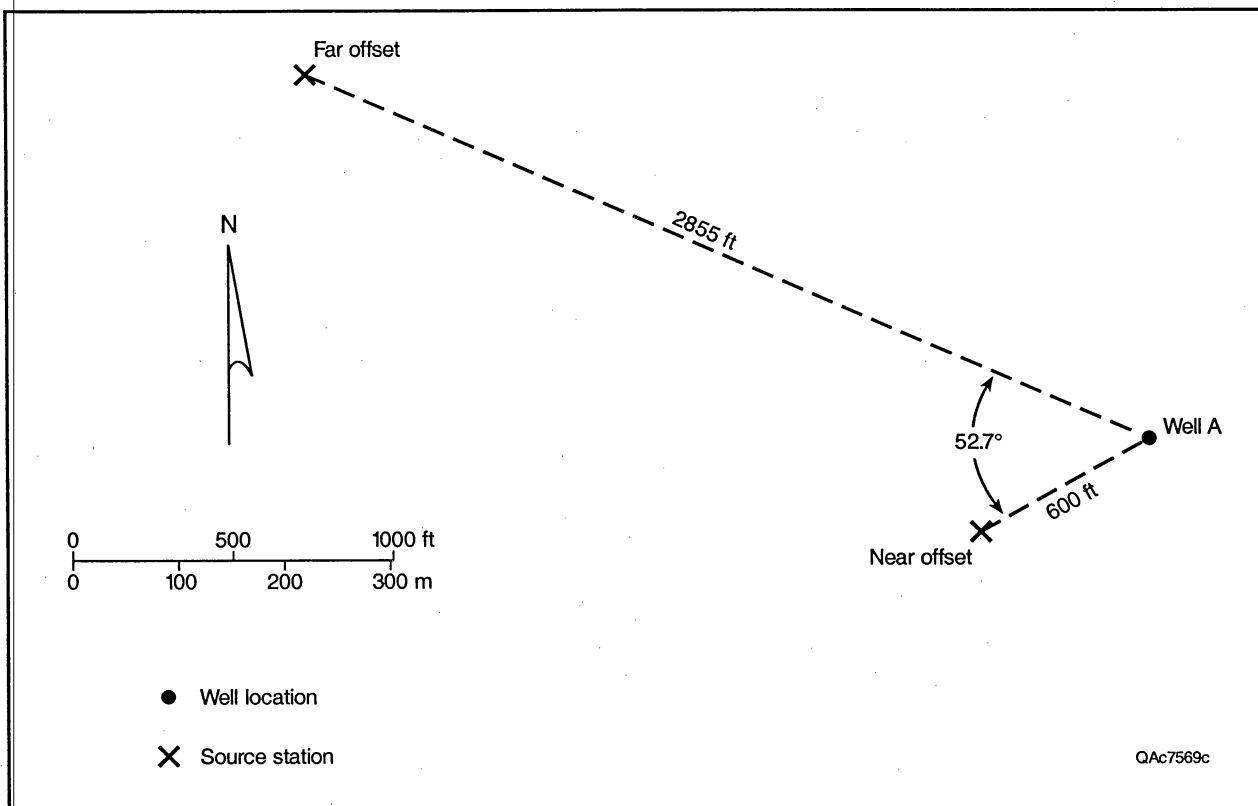
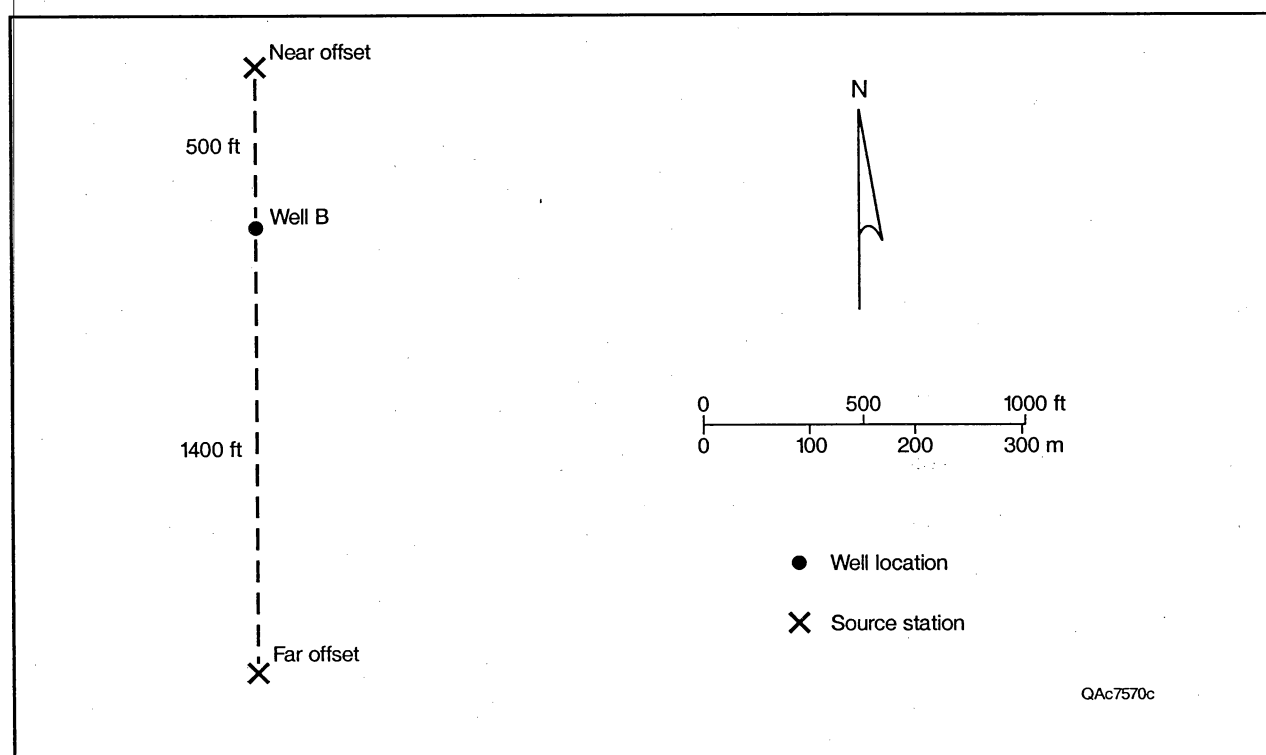Figure 7. VSP recording geometry, well A
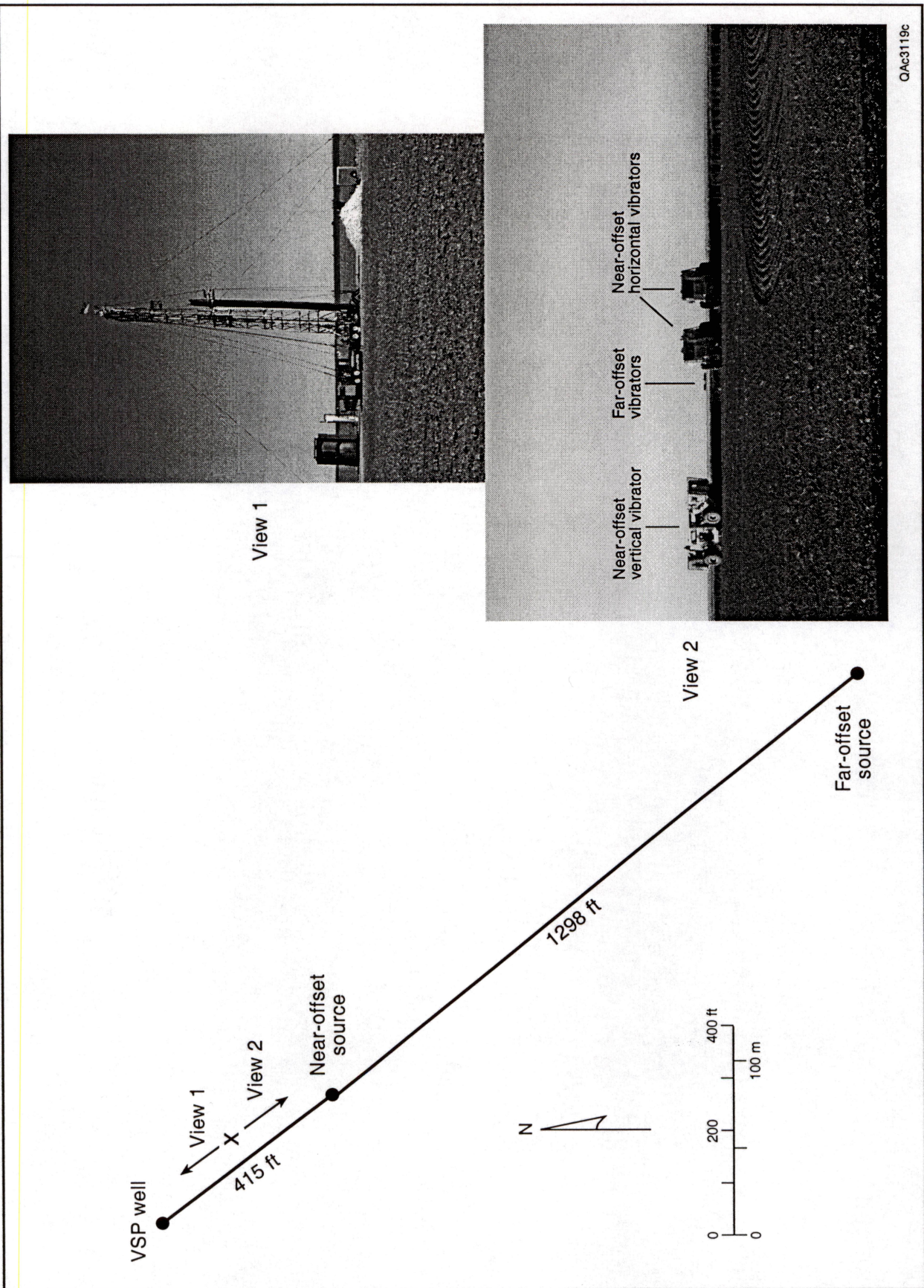

Figure 8. VSP recording geometry, well B

11

View 1

View 2

Near-offset
vertical vibrator

Far-offset
vibrators

Near-offset
horizontal vibrators

QAc3119c

VSP well

View 1

View 2

x

415 ft

Near-offset
source

1298 ft

Far-offset
source

N

0   200   400 ft

0   100 m

Figure 9. VSP recording geometry, well C. The photographs labeled View 1 and View 2 were taken at the position marked "x".

9-C VSP Data Processing

Near-offset 9-C VSP data acquired in demonstration well A are displayed in Figures 10, 11, and 12. These figures show data recorded by the V, H_1, and H_2 geophones for each vector-wavefield source positioned at the near-offset source station.

The vertical component data have reasonably good signal-to-noise character even when not rotated. If P-wave information only is what is desired, acceptable P-wave images can be made without doing the receiver rotations described in Figure 5. However, for optimal data quality, the response of the vertical geophone was rotated and is shown in Figure 10.

A different conclusion about data quality is reached when unrotated H_1 and H_2 data are examined. In each figure, the unrotated H_1 and H_2 data have inconsistent first arrivals, and amplitude and phase properties vary from trace to trace. These trace-to-trace data variations are caused almost entirely by tool spin and inconsistent orientation of the horizontal geophones as the VSP sonde is moved from depth station to depth station.

Rotated versions of the horizontal geophone data are shown in Figures 13 and 14. All three geophone channels show improved data quality, with the data improvement being particularly obvious for the horizontal receivers. A P-wave image can now be made from the V-geophone data in Figure 10; an SV-wave image can be constructed from the H_1-geophone data in Figure 13; and an SH-wave image can be produced from the H_2-geophone data in Figure 14.

Upgoing P, SH, and SV primary reflection events are labeled in each of the displays to illustrate that 9-C VSP data allow the interface where each type of reflection event is produced to be defined accurately and unambiguously. When these reflection events are separated from their respective downgoing wavefields, the resulting P, SH, and SV images can be shown as functions of stratigraphic depth. These depth-based display formats allow the images to be directly compared with well logs and depth-based engineering data.
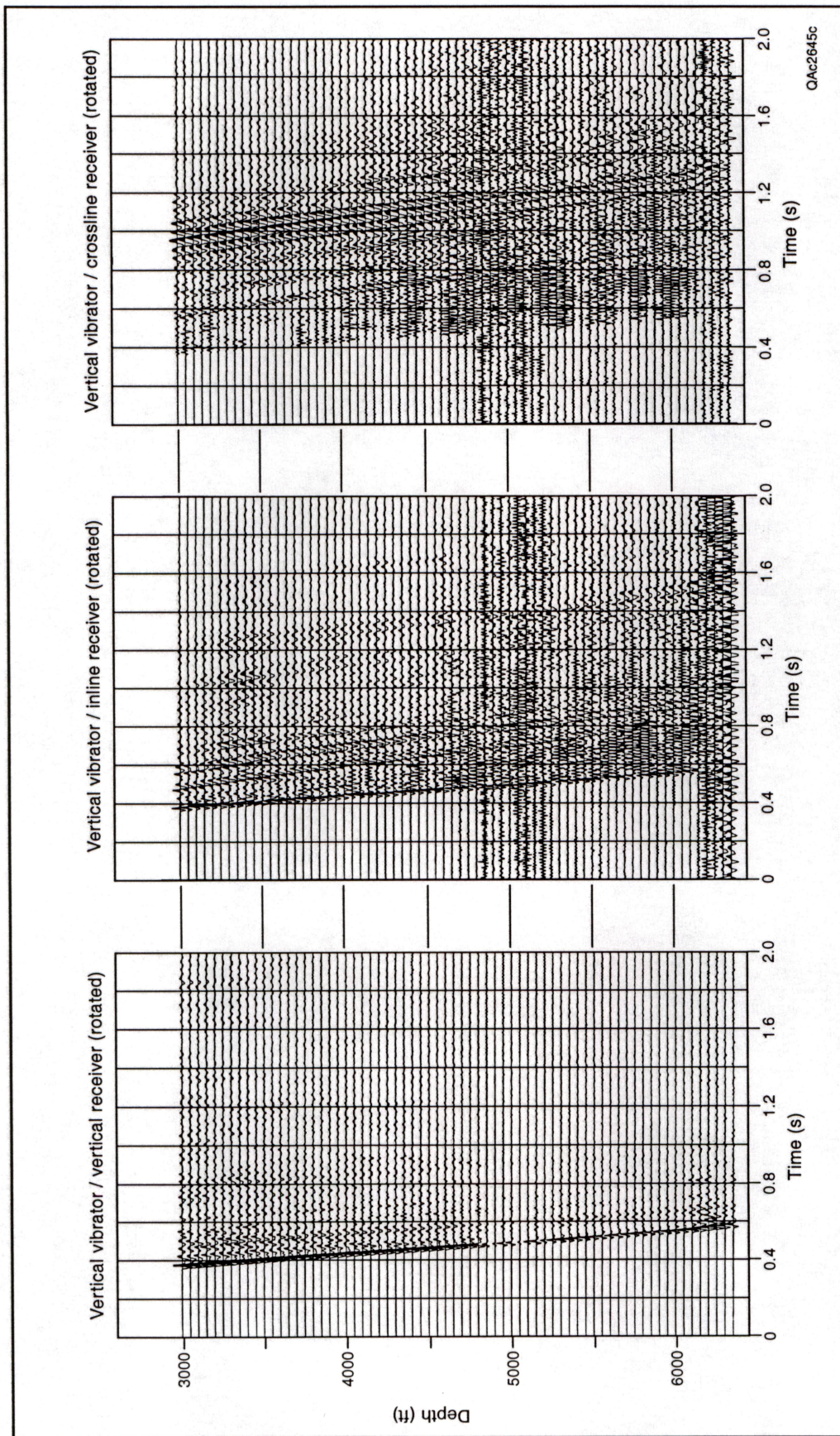
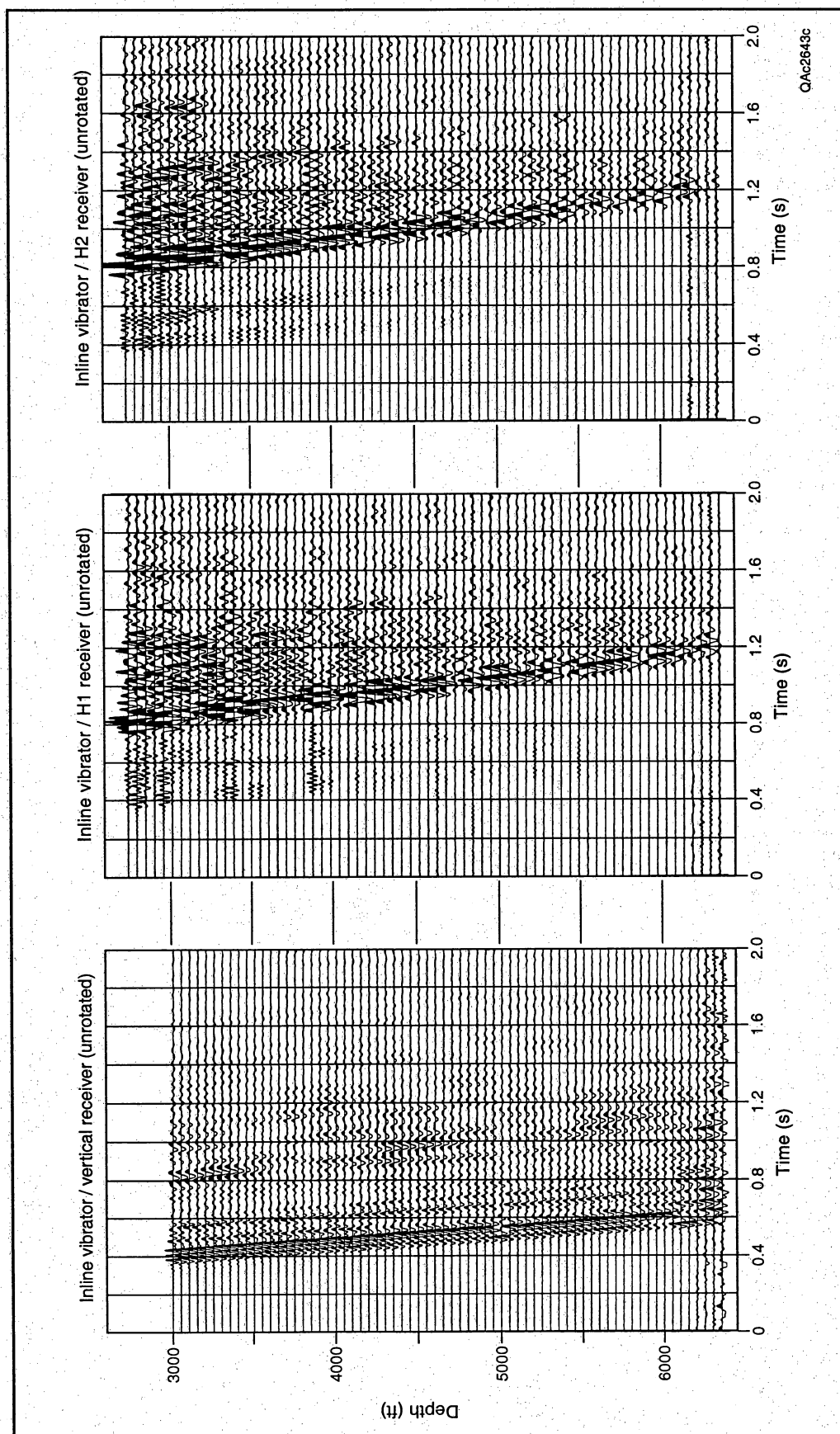Figure 10. Rotated data, vertical vibrator, well A

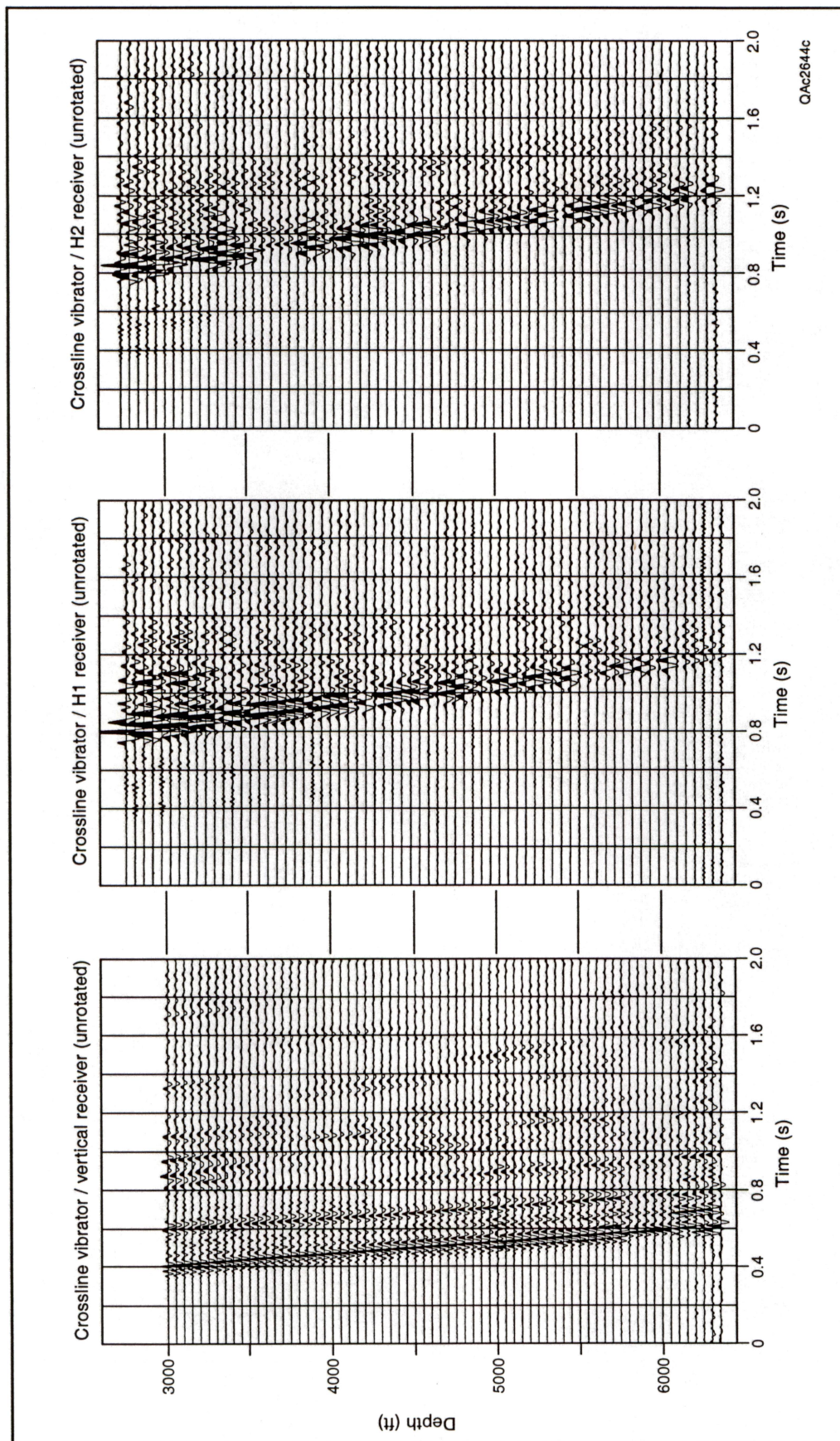Figure 11. Unrotated data, inline vibrator, well A

QAc2643c

15

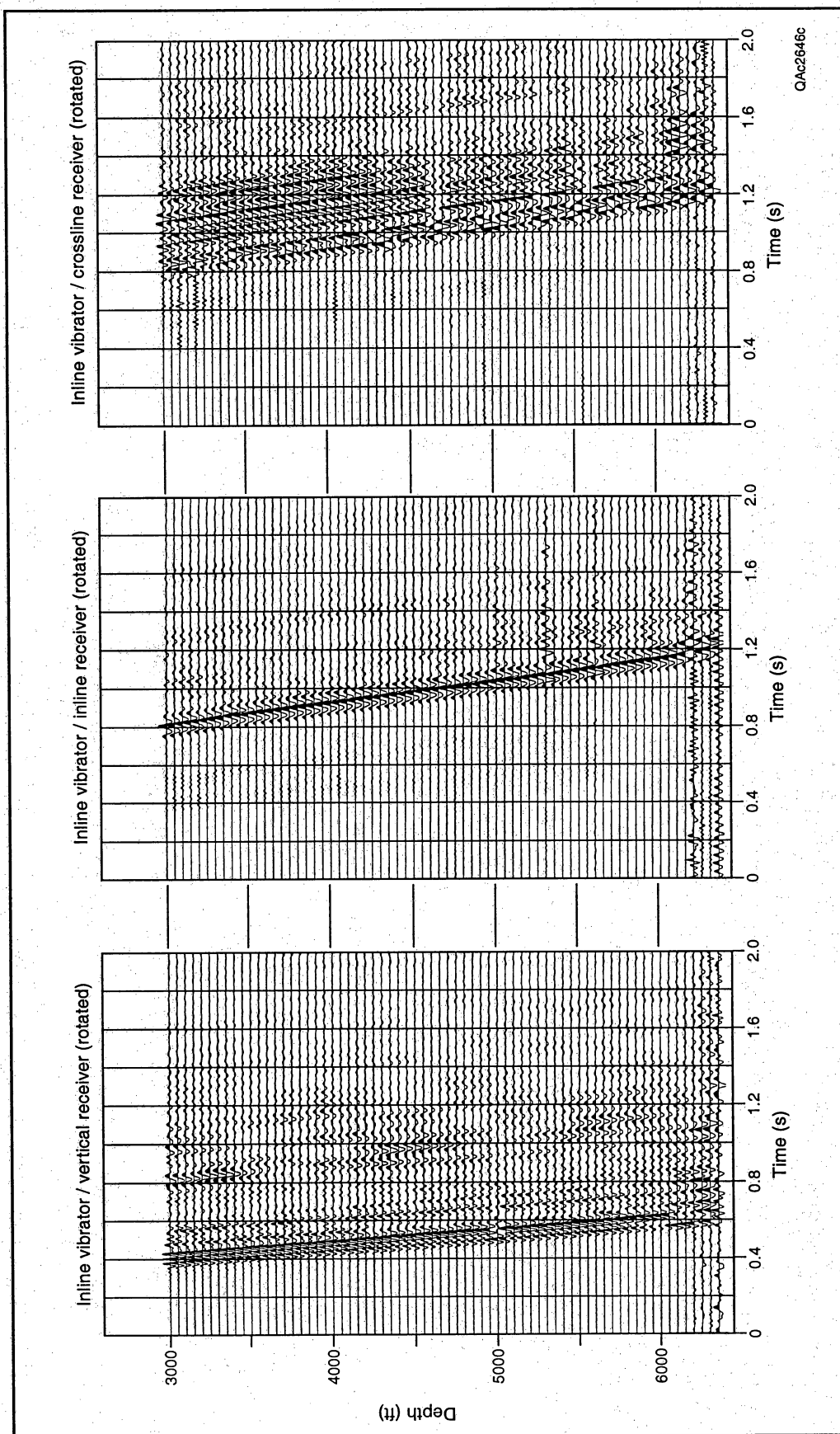Figure 12. Unrotated data, crossline vibrator, well A

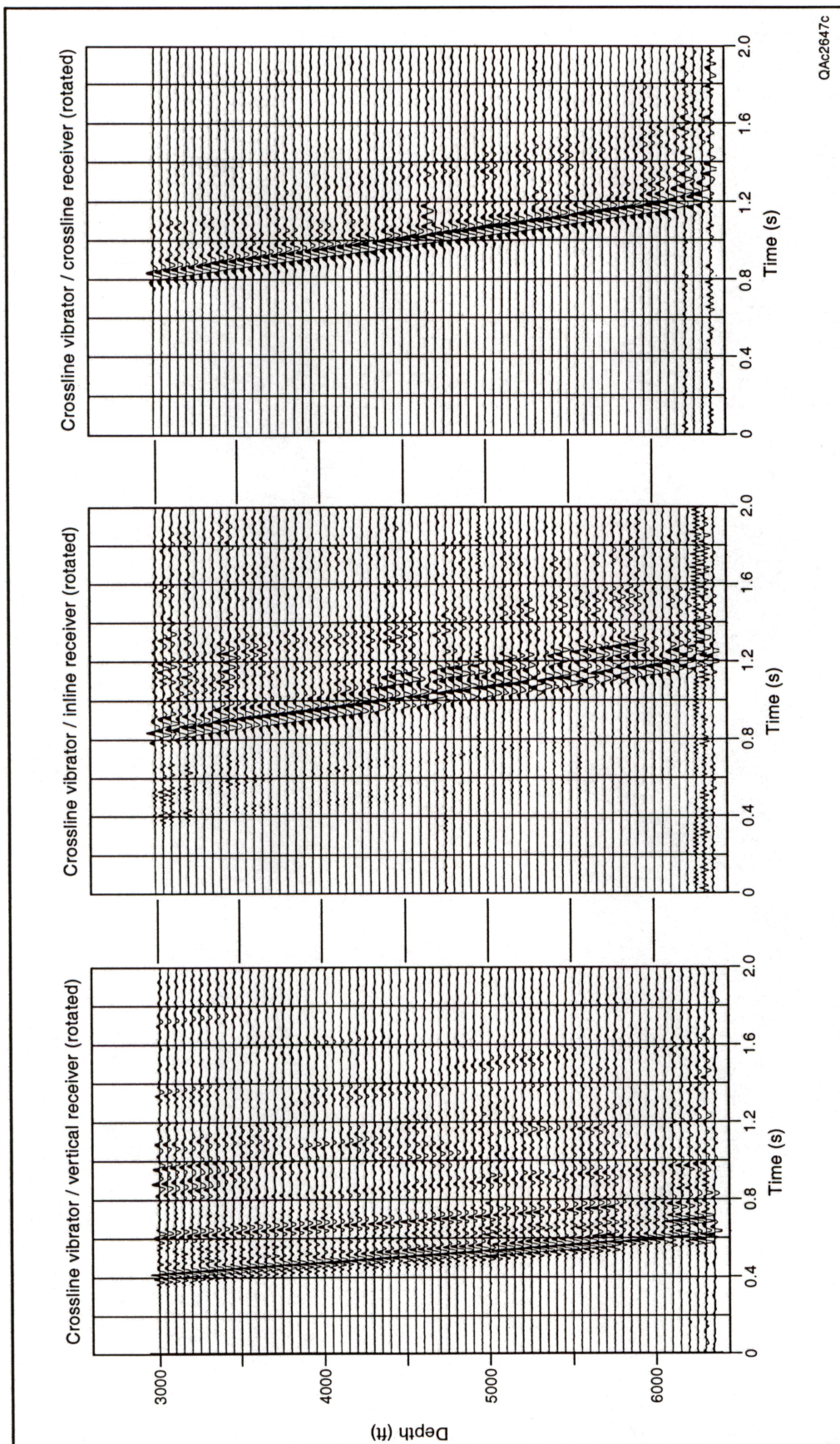Figure 13. Rotated data, inline vibrator, well A

QAc2646c

17

Figure 14. Rotated data, crossline vibrator, well A

Zero-offset P, SV, and SH images are made after the basic wavelets in the P, SV, and SH wavefields are adjusted to symmetrical, zero-phase wavelets and the rotated upgoing wavefields are deconvolved to attenuate multiples. Front-corridor stacks of wavelet-shaped, deconvolved upgoing P, SV, and SH wavefields are shown in Figures 15, 16, and 17, respectively. The resulting images can be displayed as functions of either depth or seismic image time. Depth displays were used in this study to allow easier correlation of P and S reflection character with Morrow stratigraphy.

Comparison of P and S Images with Morrow Stratigraphy

The 9-C VSP data recorded at wells A, B, and C (Fig. 1) were processed as described in the preceding section to produce depth-based, zero-offset VSP images. The P and S images created at each well are compared with Morrow log data available from those wells in Figures 18, 19, and 20.

S-wave splitting was observed at well C. Thus, the SV and SH images at this well were processed through an additional step to create S1 (fast-S) and S2 (slow-S) images. S-wave splitting was not observed at wells A and B. The data processing at these wells stopped when SV and SH images were produced.

The depth of the Morrow is labeled in each display. Examination of the figures leads to the following observations.

1.   S wave reflections are generated across the Morrow interval, as are P-wave reflections.

2.   S reflections often occur at different stratal surfaces than do P reflections. Thus improved and more detailed models of Morrow reservoir architecture should result by combining P and S seismic reflection data because a greater variety of stratal surfaces can be mapped.
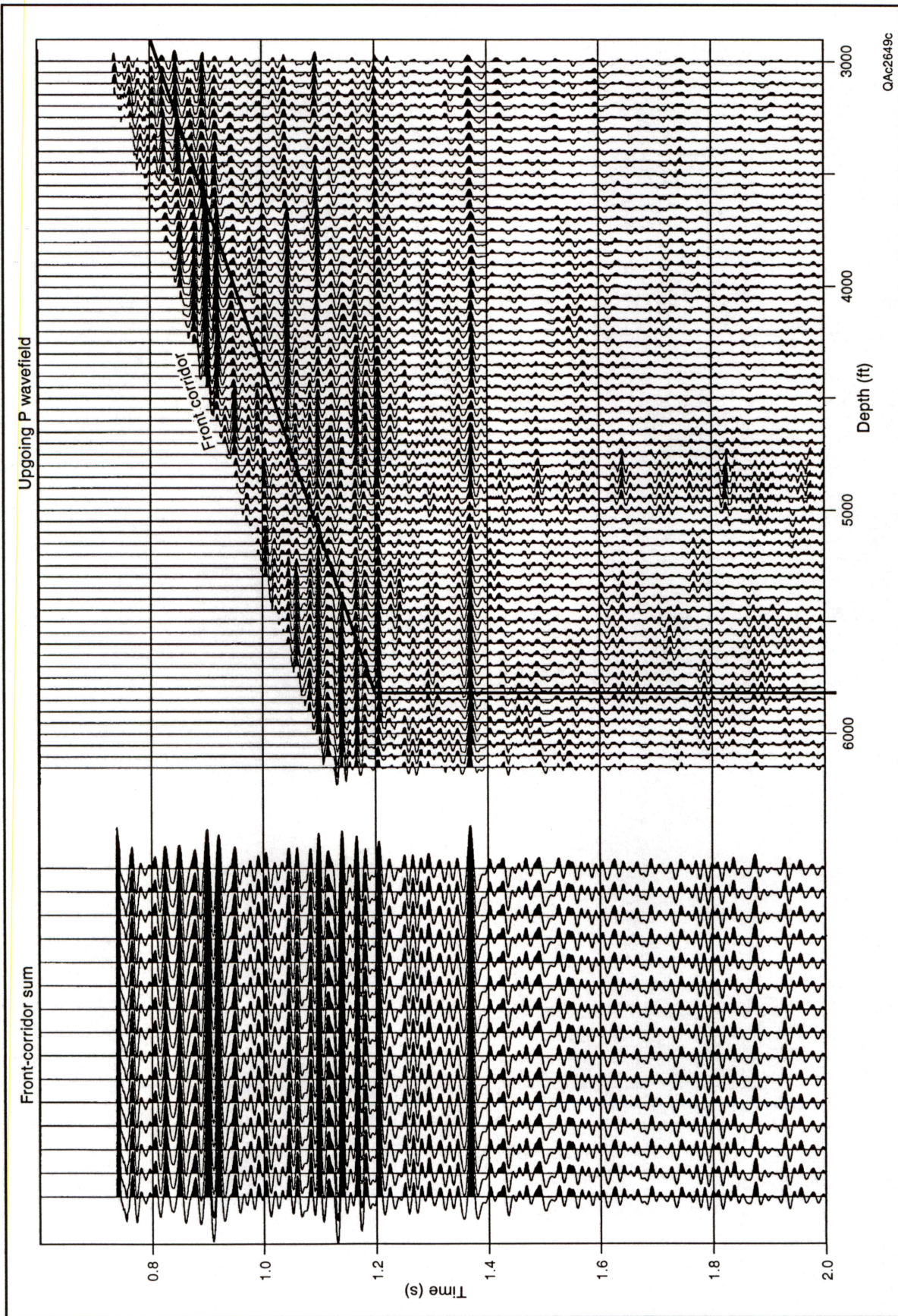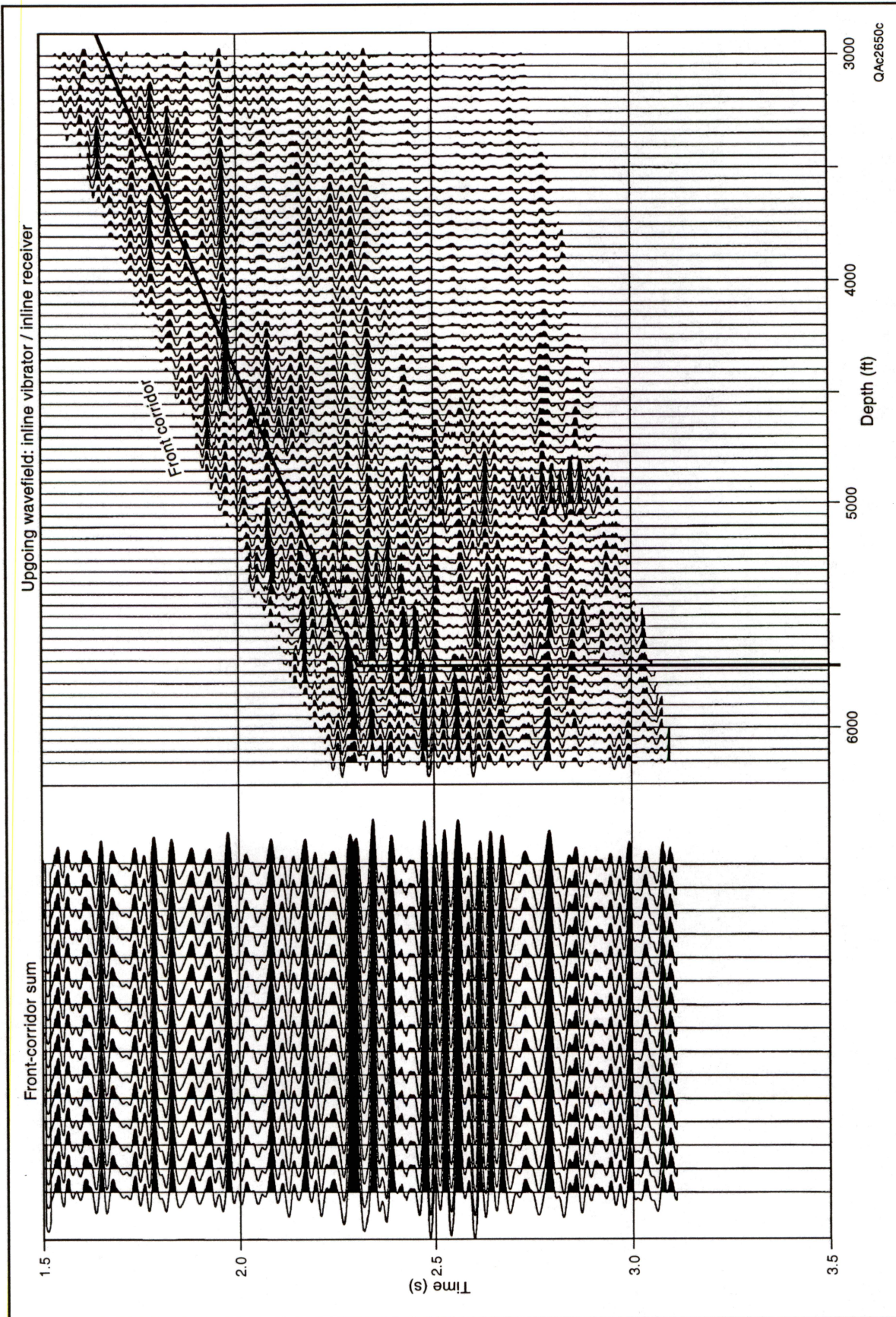
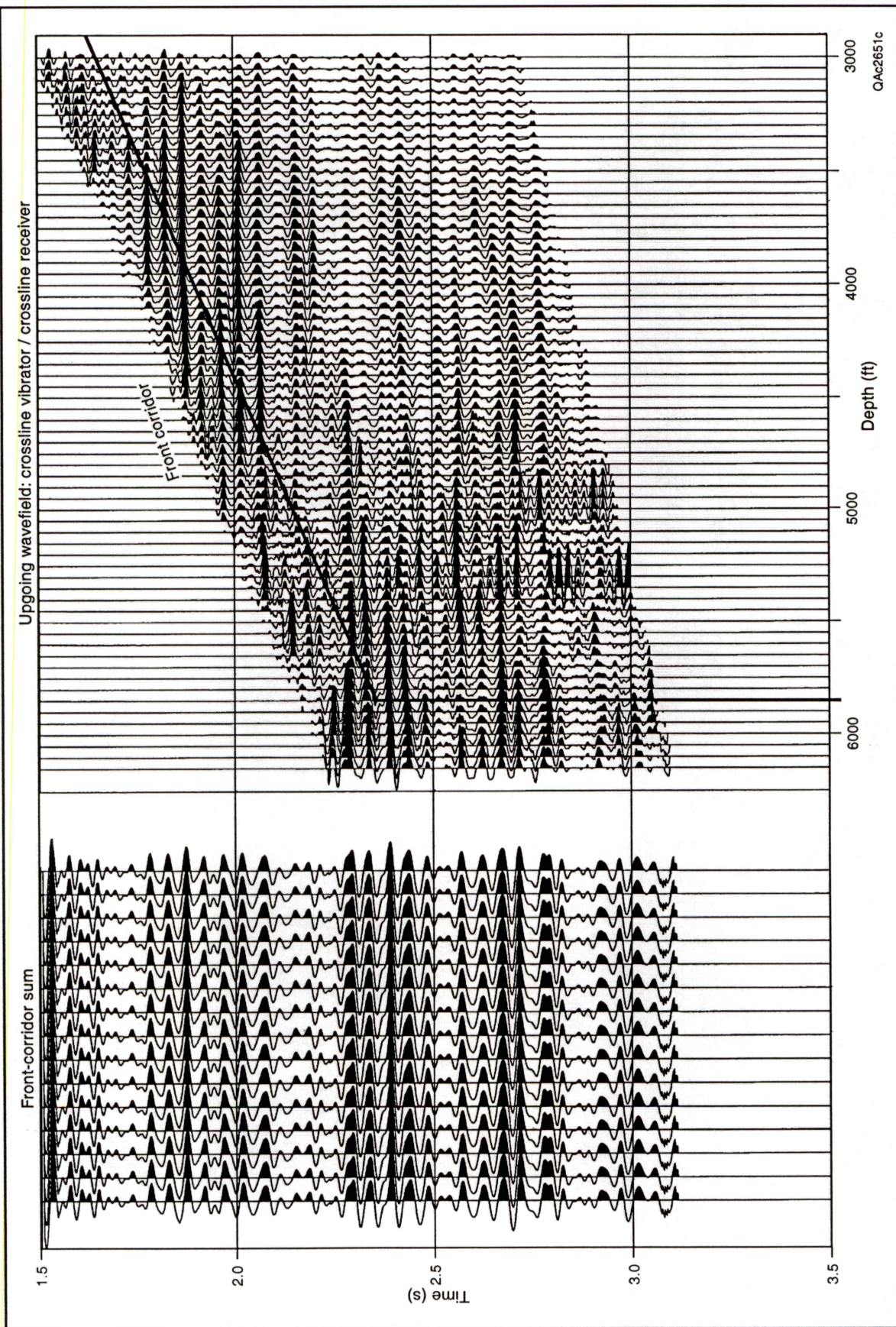Figure 15. P-wave corridor stack

Figure 16. SV corridor stack
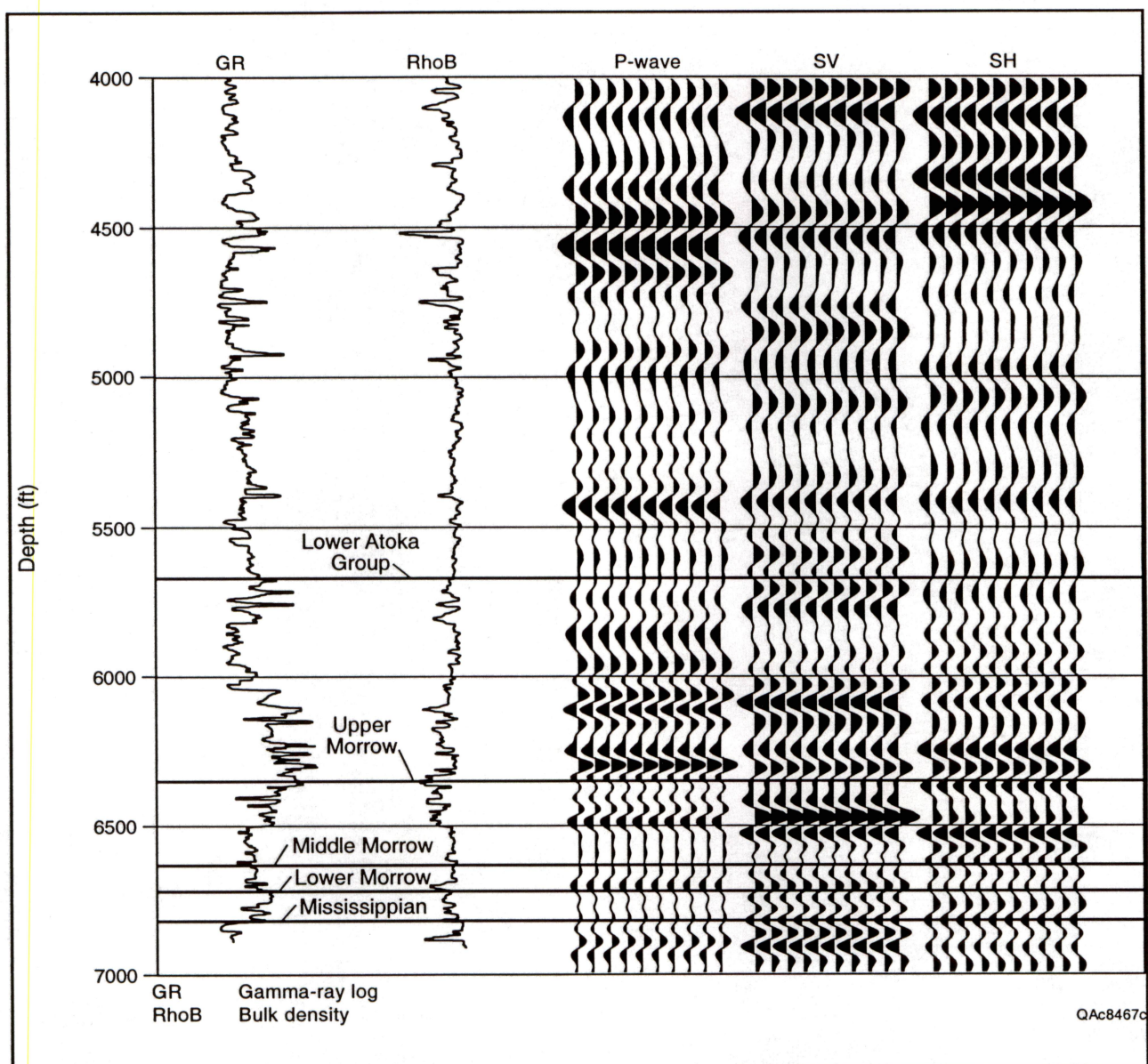
21

Figure 17. SH corridor stack

22

Figure 18. Comparison of P, SH, and SV images with well logs, well A
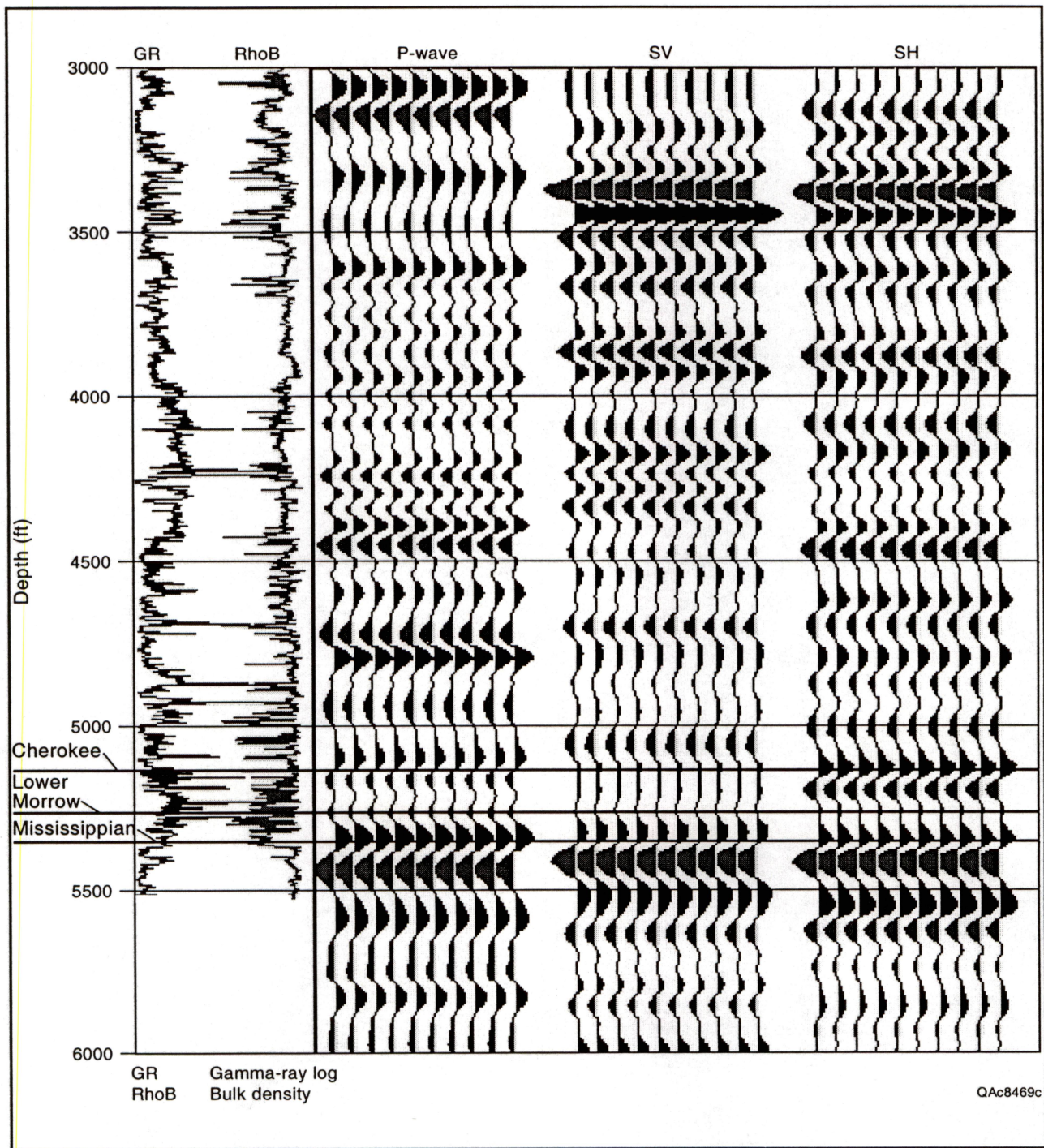
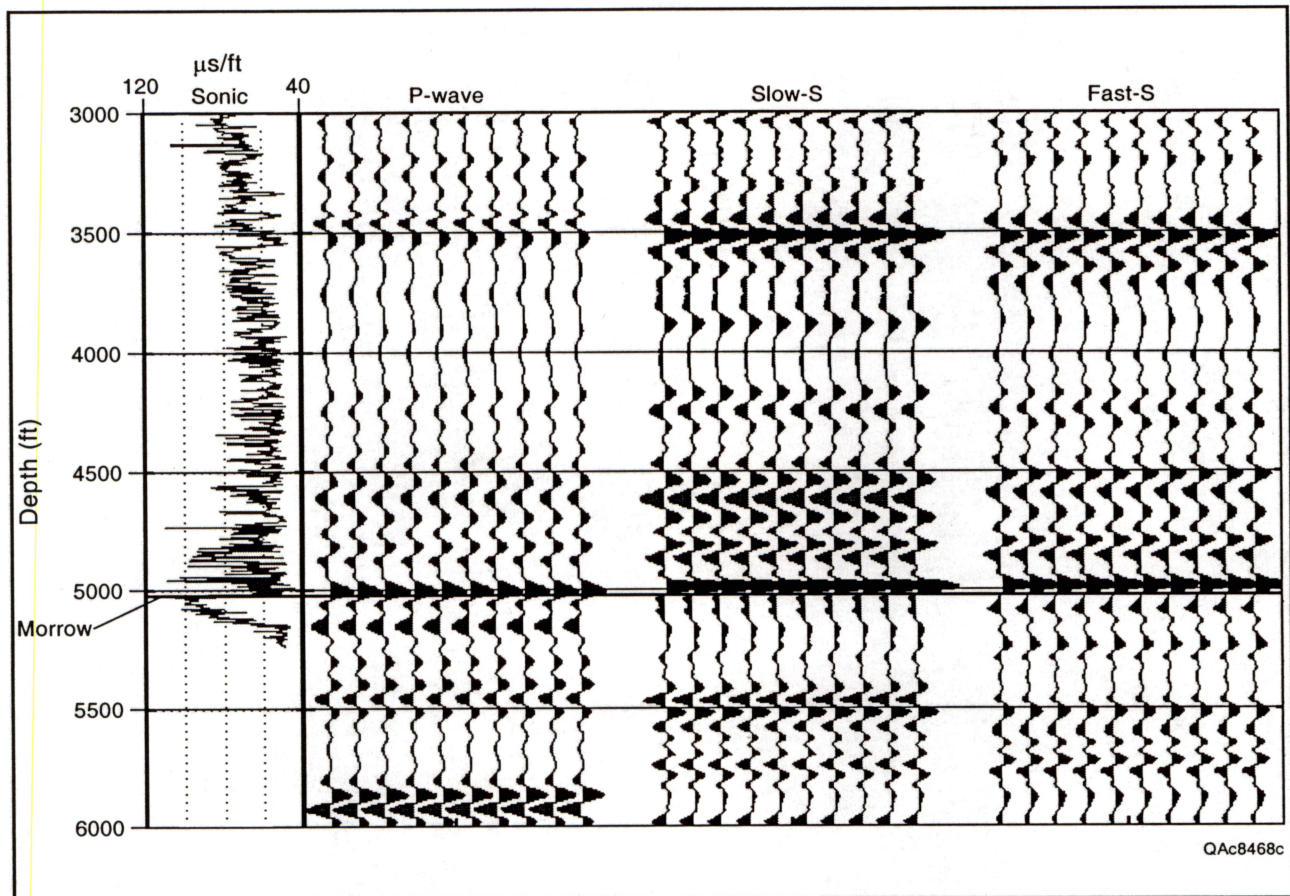Figure 19. Comparison of P, SH, and SV images with well logs, well B

Figure 20. Comparison of P, S1, and S2 images with well logs, well C

3.   In some instances, Morrow S reflections are more robust than Morrow P reflections. Examples are the SV and SH responses near depth coordinate 6,500 ft in Well A (Fig. 18), and the SH response between the Cherokee and Lower Morrow in Well B (Fig. 19). This fact suggests that S-wave seismic technology should be considered for any Morrow prospect that is difficult to image with P-wave seismic data.

4.   The vertical resolution of S-wave images constructed from 9-C VSP data is as good as the vertical resolution of P-wave images. Thus surface-recorded S-wave data should provide a spatial resolution of Morrow targets that is equivalent to the resolution achieved with P-wave surface-recorded data.

Conclusions

This study showed that Morrow reservoir targets generate good-quality S-wave reflection events. This important fact supports the premise that multi-component seismic technology can be used to create P and S images of Morrow stratigraphy.

Equally important, 9-C VSP data confirmed that S reflections often occur at different Morrow stratal surfaces than do P reflections. This reflectivity behavior means that the combination of P and S reflection images will result in improved stratigraphic interpretations of Morrow prospects. It is this fact that P and S reflections may at times follow different stratal surfaces that infers S-wave data can sometimes provide a better image of Morrow reservoirs than do P-wave data. The choice as to which wavefield, P or S, will yield the better image will depend on the specific type and sequence of stratal surfaces that exist across a prospect. Because operators rarely know what stratal surface sequences exist at a Morrow prospect, this study infers that all Morrow prospects should be evaluated with both P and S seismic data if a multi-component seismic program can be justified economically.

Perhaps the most obvious conclusion provided by this study is that 9-C VSP data should be recorded at Morrow prospects whenever possible to determine the relative imaging value of P and S data at those sites. The P and S images extracted from 9-C VSP data provide a definitive and relatively low-cost answer to the question, "Do S waves see Morrow stratigraphy better at this particular prospect than do P waves?".

References

Hardage, B. A., 2000, Vertical seismic profiling–principles: Pergamon/Elsevier Science Ltd, Amsterdam, 552 p.

Rampton, D. C., 1995, The shear difference; improved characterization of a Morrow fluvial sandstone using the shear seismic response, Sorrento Field, Southeast Colorado, Master of Science thesis, Colorado School of Mines.

Swanson, D. C., 1979, Deltaic deposits in the Pennsylvanian upper Morrow Formation of the Anadarko Basin, in Hyne, N. J., ed., Pennsylvanian sandstones of the Mod-Continent: Tulsa Geological Society Special Publication No. 1, p. 115-168.